
Q-NET: A Formula for Numerical Integration of a Shallow Feed-forward Neural Network

Kartic Subr

School of Informatics,
University of Edinburgh.
k.subr@ed.ac.uk

Abstract

Numerical integration is a computational procedure that is widely encountered across disciplines when reasoning about data. We derive a formula in closed form to calculate the multidimensional integral of functions f_w that are representable using a shallow feed-forward neural network with weights w and a sigmoid activation function. We demonstrate its applicability in estimating numerical integration of arbitrary functions f over hyper-rectangular domains in the absence of a prior. To achieve this, we first train the network to learn $f_w \approx f$ using point-samples of the integrand. We then use our formula to calculate the exact integral of the learned function f_w . Our formula operates on the weights w of the trained approximator network. We show that this formula can itself be expressed as a shallow feed-forward network, which we call a Q-NET, with w as its inputs. Although the Q-NET does not have any learnable parameters, we use this abstraction to derive a family of elegant parametric formulae that represent the marginal distributions of the input function over arbitrary subsets of input dimensions in functional form. We perform empirical evaluations of Q-NETs for integrating smooth functions as well as functions with discontinuities.

1 Introduction and background

Artificial neural networks are versatile representations of functions that have led to groundbreaking results in a variety of learning problems such as function approximation (regression), classification and dimensionality reduction. Deep neural networks have been shown to learn effective approximations of difficult functions (high-dimensional, with discontinuities, etc.) such as digital images defined over the space spanned by pixels. While there are numerous methods that focus on learning these representations, the problem of estimating integrals of the learned function remains an open problem.

In this paper, we derive a closed-form formula to calculate the integral of a specific but well known shallow feed-forward network (SFFN) containing one hidden layer and a sigmoid activation function. This textbook case is an example of what are called *universal approximator networks* [1, 2, 3] since it can approximate any continuous function $f : \mathbb{R}^d \rightarrow \mathbb{R}$ accurately [4]. Although learning one from point estimates $\{f(\mathbf{x}_n)\}$, $n = 1, \dots, N$ where $\mathbf{x}_n \in \mathbb{R}^d$ might be slow or require a large number of neurons to achieve a sufficiently accurate $f_w \approx f$, its simplicity and universality make it an attractive case to study. We derive an exact formula to describe the value of the integral of f_w as a function of the parameters or weights w learned using a standard training procedure.

A formula for integrating f_w exactly enhances its appeal as a *proxy* or surrogate function for f in applications where the latter needs to be numerically integrated. We test the utility of our formula by

estimating multidimensional integrals I and its marginals I^r , where

$$I \equiv \int_{\mathcal{D}} f(\mathbf{x}) \pi(\mathbf{x}) d\mathbf{x} \quad \text{and} \quad I^r(\mathbf{x}^{r+1, \dots, d}) \equiv \int_{\mathcal{D}_r} f(\mathbf{x}) \pi_r(\mathbf{x}^{1, \dots, r}) d\mathbf{x}^{1, \dots, r}, \quad (1)$$

over hyper-rectangular domains \mathcal{D} (d -dimensional) and \mathcal{D}_r (r -dimensional) using N samples $\{f(\mathbf{x}_n)\}$. Here π and π_r describe the distribution from which the samples are drawn in each case. Here, the superscript in $\mathbf{x} \in \mathcal{D}$ denotes select elements of \mathbf{x} , so $\mathbf{x}^{1, \dots, d} \in \mathcal{D}_r$ represents a vector with the first r components (without loss of generality) of \mathbf{x} . We focus on the case when there is no informative prior on the integrand and with π as a constant. These problems are abstract representatives of the applications of numerical integration in machine learning, e.g. normalization of multidimensional probability densities (frequentist statistics) or likelihood functions (likelihood statistics), computation of marginal likelihoods (model evidence) which forms the crux of Bayesian approaches, etc. An advantage of the surrogate function over averaging of point samples (ala Monte Carlo integration) is that it enables functional representations of marginal distributions. Another advantage is that f_w might be used as a control variate [5, Sec. 8.9][6] as shown in section 3.

Despite the plethora of computational approaches such as quadrature rules [7, 8], Monte Carlo integration and Markov Chain Monte Carlo methods, the general procedure to estimate integrals of functions using point samples remains frustratingly inefficient even in moderately many (about ten) dimensions. Monte Carlo methods operate by expressing integrals as expectations which can be estimated via random simulation [9]. Several variants of this method address its slow $O(1/\sqrt{N})$ convergence, and strike different compromises between *bias* (accuracy) and *variance* (precision). We refer the reader to standard texts on the subject [5]. Quasi-Monte Carlo (QMC) methods replace stochasticity with carefully designed, deterministic samples which improves convergence dramatically when the integrands are smooth [10, 11] or of moderate dimensionality (below ten). Deep neural networks can mimic MC solutions to certain partial differential equations [12] sidestepping the curse of dimensionality.

Bayesian methods use probabilistic model-based surrogates to improve sample-efficiency for expensive integrands [13] or to guide active sampling (adaptive Bayesian quadrature [14, 15], Bayesian Optimization [16], etc.). This general approach can be used to estimate the marginal likelihood [17, 18], approximate the posterior [19, 20] and to simultaneously infer both [21]. These works impose a Gaussian Process (GP) prior on the integrand and focus on cases where analytical formulae can be derived for the expectation and uncertainty of the statistical surrogate. The non-parametric nature of the GP can affect scalability and the need to explicitly evaluate the sampling probability sometimes precludes the use of these methods. The advantages of these approaches is that they inherently enable reasoning about uncertainty and that they serve as generative models. Hybrid methods such as using GPs to model weights [22] investigate calibrated reasoning about uncertainty using probabilistic neural networks. *Integral representations* [23] use an analysis of continuous distributions, for a particular target function, from which instances of shallow neural networks can be sampled.

We test the utility of a neural network as a surrogate representation for numerical integration. We identify that the integral of a sigmoidal universal approximator function can be expressed in closed form and derive its formula. Our result can be viewed as parametric in the sense that for a fixed architecture, the set of parameters (weights and biases) learned is independent of the amount of training data. Once learned, a parametric formula can be used to evaluate the integral or its marginals. On the other hand, it does not encode distributional information or serve as a generative model.

Contributions The contributions of this paper are:

1. a formula, to estimate multidimensional integrals of f_w , a neural network function representation;
2. an interpretation of the formula as a neural network with one hidden layer which we call a Q-NET;
3. and a parametric formula for marginalization of f_w along subsets of input dimensions.

We test the use of f_w for approximate numerical integration using smooth and discontinuous functions.

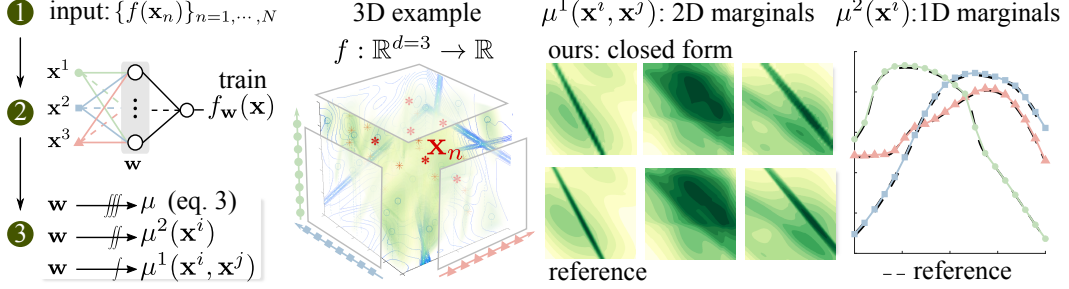


Figure 1: *Overview*: We derive a formula in closed-form to integrate a function f_w represented using a shallow, feed-forward sigmoidal network. Once f_w is trained as a proxy to some function f using samples $f(\mathbf{x}_n)$, the formula can be used to approximately integrate or marginalize f . Here, it is applied to marginalize the pdf of a Gaussian mixture in 3D (visualized) along different axes to obtain accurate parametric (functions of \mathbf{w}) formulae for the 2D and 1D marginal distributions.

2 Numerical integration of a shallow feed-forward network

2.1 Preliminaries

We denote row¹ and column vectors with boldface characters (e.g. \mathbf{x} , \mathbf{b}_1 , \mathbf{w}_2) and capital letters to represent matrices (e.g. W_1). Superscripts denote selected elements of a vector or matrix. So \mathbf{b}_1^i and $W_1^{i,:}$ represent the i^{th} element \mathbf{b}_1 and i^{th} row of W_1 respectively. For convenience, we will operate in a normalised domain $\mathbf{x} \in \mathcal{D} \equiv [-1, 1]^d$, as is commonly the case with inputs of neural networks. General hyper-rectangular domains may be handled by scaling the dimensions independently (see Sec.4). We use $f_w : [-1, 1]^d \rightarrow \mathbb{R}$ to represent an approximation of the function f obtained by training a shallow feedforward neural network with one hidden layer of k neurons and a linear output layer using N samples $f(\mathbf{x}_n)$ $n = 1, \dots, N$. For convenience, we use \mathbf{w} to collectively encode all learnable parameters of the approximator network: a $k \times d$ matrix W_1 , a k -dimensional row vector \mathbf{w}_2 , a k -dimensional column vector \mathbf{b}_1 and a real number b_2 . The approximate function f_w is

$$f_w(\mathbf{x}) = \mathbf{w}_2 \cdot \sigma(W_1 \mathbf{x} + \mathbf{b}_1) + b_2, \quad (2)$$

where we define σ to be the logistic function that operates independently on each of the k elements of the input: $\sigma^i(\mathbf{z}^i) \equiv 1/(1 + e^{-\mathbf{z}^i})$. In this case, we derive a closed-form formula $\mu_{d,k}(\mathbf{w})$ that exactly computes $\int_{\mathcal{D}} f_w(\mathbf{x}) d\mathbf{x}$ as an approximation to I (eq. 1) and show that the formula can be adapted to produce a closed-form representation of its marginals I^r (eq. 1).

2.2 The formula

Our formula for the d -D integral of f_w using k neurons is (see App. A.1)

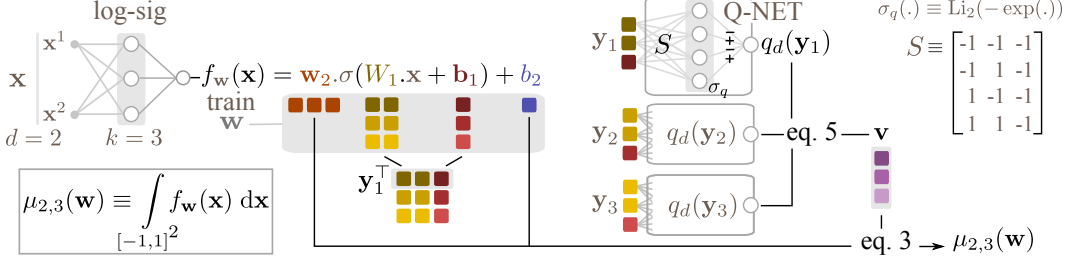
$$\mu_{d,k}(\mathbf{w}) = \mathbf{w}_2 \cdot \mathbf{v} + 2^d b_2 \quad (3)$$

$$\text{where } \mathbf{v}^i = 2^d + \frac{1}{\prod_{j=1}^d W_1^{i,j}} \sum_{m=1}^{2^d} (-1)^{\alpha_m} \text{Li}_d \left(-\exp(S^{m,:} W_1^{i,:} - \mathbf{b}_1^i) \right). \quad (4)$$

Here $\text{Li}_d(x)$ represents the polylogarithm [24, 25] function of order d and S is a ‘sign’ matrix with elements in $\{-1, 1\}$ whose 2^d rows represent all combinations of d signs. The contribution of each Li_d term is positive (or negative) depending on α_m , which is even (resp. odd) when there is an even (resp. odd) number of -1 s in the row $S^{m,:}$. \mathbf{v} is a column vector whose elements correspond to the outputs of each of the neurons in the hidden layer.

The computational complexity of evaluating the formula is $O(k d 2^d)$ and the memory complexity is $O(kd + d^2)$ since the columns of the elements of S can be binary encoded with length $O(d)$. While the computation time is independent of the number of samples of the integrand N , increasing N improves f_w as an approximation of f .

¹We do not assume that all vectors are column vectors so that the formulae in the paper match output weights of neural network libraries with no extra transposes necessary for implementation.



2.3 Q-NET representation

Although calculation can be performed explicitly as in equations 3 and 4, we observe that the expression within the summation term may itself be represented using a feedforward neural network, with one hidden layer containing 2^d neurons, which we call Q-NET. The parameters (weights, biases and activation function) of the Q-NET are fixed (not learned) as a function of d and independent of the parameters of w . The input to the Q-NET is a concatenation of a row of the weight matrix W_1 and the corresponding bias term: $\mathbf{y}_i \equiv [W_1^{i,:} \ b_1^i]^\top$. The first layer is defined by weight matrix that is S concatenated with a column of -1 s, $[S \ -\mathbf{1}_{2^d}]$, and zero bias. The activation function for the hidden layer is $\sigma_q(\cdot) \equiv \text{Li}_d(-\exp(\cdot))$ and the output is a linear combination with weights $+1$ for those neurons whose input weights contain an odd number (since we concatenated $-b_1^i$ to each row) of -1 s and -1 otherwise. to with zero bias. Thus, the output of the Q-NET is $q_d(\mathbf{y}_i) \equiv \sum_{m=1}^{2^d} (-1)^{\alpha_m} \sigma_q(S^{m,:} W_1^{i,:} - b_1^i)$. The subscript serves as a reminder that the Q-NET is fully specified by d . Now eq. 4 simplifies to

$$\mathbf{v}^i \equiv 2^d + q_d(\mathbf{y}_i) / \prod_{j=1}^d W_1^{i,j} \quad (5)$$

so that the i^{th} element of the column vector \mathbf{v} is calculated using a single evaluation of the Q-NET: $q_d(\mathbf{y}_i)$. Figure 2 provides an illustrative summary of how QNETs may be constructed and used. The output of the Q-NET (eq. 5) is identical to the formula in eq. 4. While it might be possible to construct a single network whose output is $\mu_{d,k}$, this would be complicated by the denominator in \mathbf{v}^i . Although the Q-NET does not have any learnable parameters, it is a useful abstraction for $\mu_{d,k}$ that enables an elegant representation of integrals along sub-dimensions (marginalization).

2.4 Marginalizing using Q-NETS

We now explain how $r < d$ dimensions of \mathbf{x} may be marginalized. Although we choose the first r adjacent dimensions $\mathbf{x}^{1,\dots,r}$ for convenient exposition the following procedure holds without loss of generalization for any r dimensions of \mathbf{x} . The result of marginalizing these dimensions is a function $\mu_{d,k}^r(\mathbf{w}, \mathbf{x}^{r+1,\dots,d})$ whose formula requires integration over r dimensions. Using Q-NETs, we obtain:

$$\mu_{d,k}^r(\mathbf{w}, \mathbf{x}^{r+1,\dots,d}) = \mathbf{w}_2 \tilde{\mathbf{v}} + 2^r b_2 \quad \text{where} \quad \tilde{\mathbf{v}}^i \equiv 2^r + q_r(\tilde{\mathbf{y}}_i) / \prod_{j=1}^r W_1^{i,j} \quad (6)$$

where the only differences from equation 5 are: 1) that d has been replaced with r on the rhs ; and 2) that the input to the Q-NET is $\tilde{\mathbf{y}}_i \equiv [W_1^{i,1,\dots,r} (b_1^i + W_1^{i,r+1,\dots,d} \mathbf{x}^{r+1,\dots,d})]^\top$ instead of \mathbf{y}_i . In other words, the weighted non-marginalized variables are added to the last column of \mathbf{y}_i to obtain $\tilde{\mathbf{y}}_i$. Thus, by modifying the input and evaluating Q-NET (parameterized by the reduced dimensionality) we can approximate marginal distributions. Our definition of Q-NETs is motivated by this ability to elegantly obtain functional approximations to marginal distributions from point-sampled functions. See figure 3 for an illustrative summary and figure 1 for an example. The example shows the result of integrating a 3D function (Gaussian mixture with 35 components) using $k = 35$ neurons in the hidden layer and $N = 2048$ samples. The figure drops subscripts on μ for brevity. Also shown are the point-sampled functions for μ^1 and μ^2 for different permutations of the components of \mathbf{x} . In other words, different marginals in 2D and 1D.

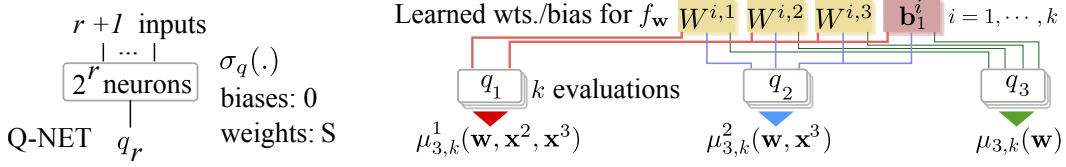


Figure 3: The figure shows how a Q-NET (left) may be applied to the weights of f_w with $r = 1, 2, 3$ to obtain parametric functions $\mu_{3,k}^r$ (right) as the different marginal distributions of $f_w(\mathbf{x})$, $\mathbf{x} \in \mathbb{R}^3$.

3 Empirical evaluation

The empirical results in this section demonstrate that: 1) error consistently diminishes with increased training samples for moderate dimensionality ($d < 12$); 2) the approach is applicable for challenging classes of integrands in the absence of any prior; and 3) that f_w can be used as a control variate, which improves on standard MC and QMC on discontinuous integrands for d as low as 4.

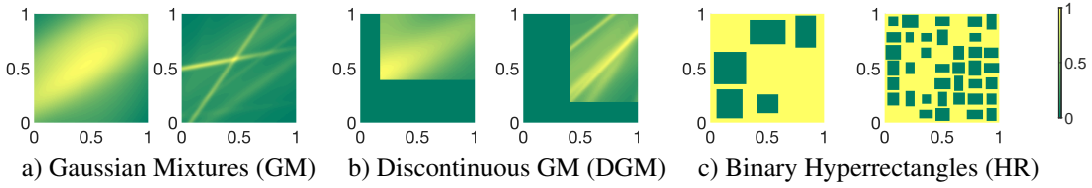


Figure 4: 2D Examples of randomly generated integrands used: a) Gaussian mixture, b) Gaussian mixture with discontinuities at d hyperplanes and c) a binary integrand that is one everywhere except inside randomly located hyperrectangles.

We trained f_w using samples from three families of integrands. The first, GM, is the probability density function (pdf) of a mixture of Gaussians parametrized by dimensionality d and the number of components in the mixture. The covariances are generated randomly, in a way that the Gaussians become narrower (peaky) as the number of components is increased. Figure 4. a visualizes two examples in 2D with 5 and 25 components. The second class GMD is the same as GM but with discontinuities introduced. We choose a random point \mathbf{x}_0 in the domain and zero out the pdf of GM if there exists i such that $\mathbf{x}_0^i > \mathbf{x}^i$. Everywhere else it is identical to GM (see fig. 4. b). The third family of integrands HR is a binary function equals one everywhere except within a set of randomly located and sized (but centered on a grid) hyper-rectangles where the function is zero. The parameters are dimensionality, number of grid cells per axis and the fraction of the total grid-cells that are chosen. e.g. setting the parameters to 8, 3 and 0.5 will result in $\text{ceil}(0.5 * 3^8) = 329$ randomly sized boxes, whose centers are unique, on a grid with 3^8 cells. All computation was performed using an unoptimized MATLAB implementation and executed (CPU only) on a standard desktop machine (single 4 core processor) with 32GB RAM. It takes about one second to obtain an estimate in 12D.

Convergence tests We averaged the relative root mean-squared error (RRMSE) of our N -sample estimates 60 times each across 120 randomly generated integrands for $N = 16, 128, 512, 1024, 2048$. We use RRMSE since each instance of the integrand has a different reference integral. We plotted the mean and standard deviation (error bars) of RRMSE against N on a log-log scale for $d = 2$ (fig. 5 top row) and $d = 5$ (fig. 6 top row). Error-bars depict variability across integrands. We plotted the relative variances or the estimator (sample variance divided by the square of the reference value) for $d = 2$ (fig. 5 bottom row) and $d = 5$ (fig. 6 bottom row). The graphs show the statistics of a standard MC estimator (grey) and a QMC (black) estimator using Halton samples alongside ours (red). Dashed trend lines $O(N^{-0.5})$ and $O(N^{-1.5})$ are also shown for RRMSE (squares for variance).

The plots show that RRMSE consistently decreases as N is increased. Curiously, for $d < 5$, Q-NET converges faster than MC despite training with random samples \mathbf{x}_n . For discontinuous f in higher dimensions, using f_w results in higher error as predicted by theory (see sec. 4). For each N sample estimator, the statistics of MC and QMC estimators were calculated using $60 \times 120 \times N$ evaluations of the integrand. On the other hand, *ours only requires N evaluations* since 7200 different estimates are obtained by stochasticity in training and initialization. This could be relevant when sampling f .

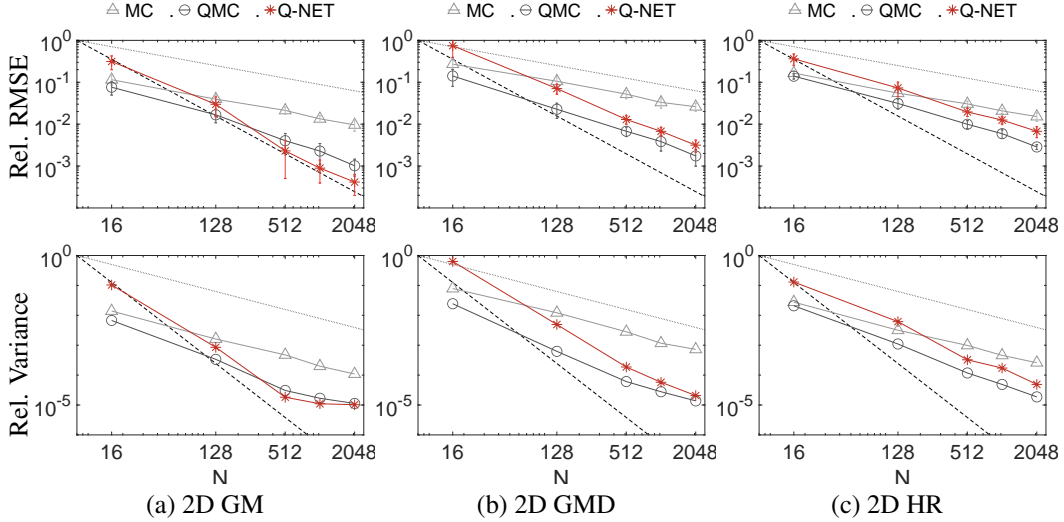


Figure 5: Convergence plots for relative RMSE (top row) and relative variance (bottom) averaged across randomly generated 2D integrands from three families (columns). Ours is shown alongside MC and QMC references (solid grey) and error trend lines (dashed grey) for $O(N^{-0.5})$ and $O(N^{-1.5})$.

repeatedly is prohibitively costly, or even impossible, as could be the case in some real problems such as those involving large amounts of computation (e.g. astronomy), surveys or clinical trials.

Control variates We devised a family of estimators CV-Q-NET, parametrized by $\nu \in [0, 1]$, that use f_w as a control variate [5, Sec. 8.9] to integrate f rather than as a direct proxy. Given ν , CV-Q-NET uses $\text{ceil}[(1 - \nu)N]$ samples to train f_w and the remaining samples to integrate $f_\Delta(\mathbf{x}) = f(\mathbf{x}) - f_w(\mathbf{x})$ via standard MC or QMC. The final estimator is then the sum of the closed-form integral of f_w and the MC (or QMC) estimator. When $\nu = 0$, CV-Q-NET is equivalent to μ (Q-NET) and as ν tends to one it approaches pure MC (or QMC). The results (fig. 7) show a dramatic reduction in variance for intermediate values of ν .

Dimensionality and nature of the integrand Since existing theoretical results (see sec. 4) for error do not apply to non-bandlimited functions such as HR, we provide empirical results of relative

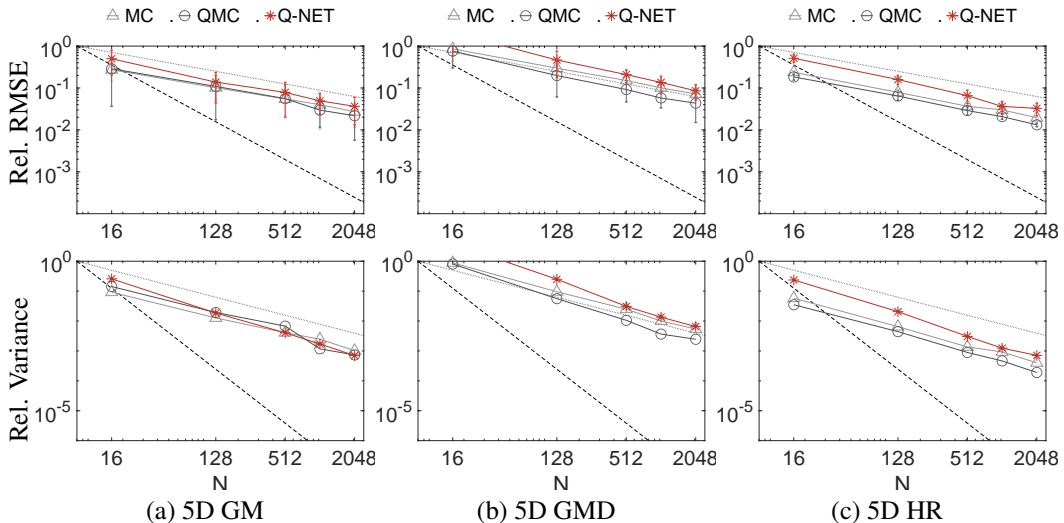


Figure 6: Convergence plots for relative RMSE (top row) and relative variance (bottom) averaged across randomly generated 5D integrands from three families (columns). Ours is shown alongside MC and QMC references (solid grey) and error trend lines (dashed grey) for $O(N^{-0.5})$ and $O(N^{-1.5})$.

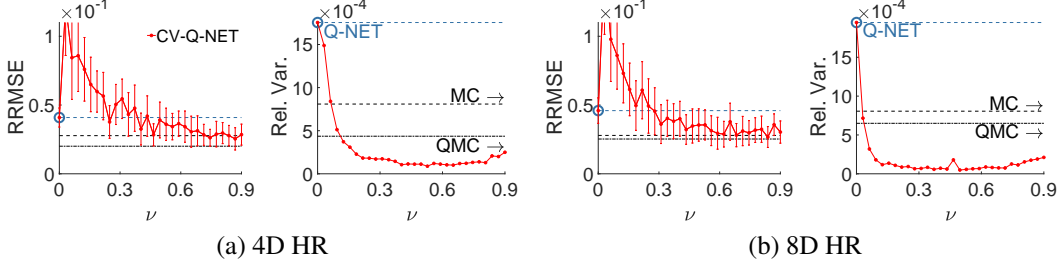


Figure 7: *Control variates* We used a fraction ν (X-axes) of the training samples $N = 512$ to randomly sample the domain and the remaining samples to build the proxy f_w which we used as a control variate. We call this estimator CV-Q-NET, which is equivalent to Q-NET when $\nu = 0$ and equivalent to MC (or QMC) when $\nu = 1$. For values $0 < \nu < 1$, we see that RRMSE reduces to MC. The variance curves show dramatic reductions particularly when ν is around 0.5. We used 40 and 60 random HR integrands to estimate the means, error-bars and variances in 4D and 8 respectively.

error (fig. 8.a) and variance (fig. 8.b) across dimensions 2, 3, 5, 6, 8 and 12 for different volumes of training data N (different curves). Although there is an increase in error from dimensions 2 to 5 (consistent with the convergence plots), reassuringly, this effect diminishes for the higher dimensions even for this challenging class of integrand. We also investigated the effects (on error) of increasing variation of f within \mathcal{D} via input parameters in GMD (number of components) and HR (number of hyper-rectangles). Figure 9 visualizes the relative error and variance of our estimator using $N = 1024$ training samples and with different numbers of neurons k (different lines). The results were obtained by averaging across 60 randomly generated integrands and from each family and the variation across the integrands is visualized as error bars. For GM, the error increases slightly for more components but for HR it remains constant. Curiously, in both cases the variance is higher while using more neurons. We found the cause to be ‘ringing’ artifacts in f_w at the discontinuities when k is large.

4 Discussion

Error The error of sigmoidal universal approximator networks [26, 4] is bounded by ϵ which is proportional to the first moment of the Fourier spectrum of f and inversely proportional to $k^{\frac{2c}{d}}$ when f is c times differentiable. From this, the error of our estimator μ can be bounded as $(I - \mu)^2 < \epsilon - V[f - f_w]$ (derived in App. A.2). Compared to reconstruction, numerical integration requires a factor of 2^d fewer samples [27, 28] (below the Nyquist rate).

Domain and range adjustment Our formula is derived assuming a normalized domain of $[-1, 1]^d$ and range of $[0, 1]$ for the approximator network. However, our test integrands are in $[0, 1]^d$ with unknown range. It is easy to show (using elementary variable substitution) that an estimate $\hat{\mu}_{d,k}$ in the normalized space can be transformed to an estimate $\mu_{d,k}$ in an arbitrary domain $[\mathbf{x}_a, \mathbf{x}_b]$ for a function with range $[z_a, z_b]$ using the formula $\mu_{d,k} = \Omega \cdot [(z_b - z_a)(\hat{\mu}_{d,k}/2^d + 1)/2 + z_a]$, where $\Omega = \prod_{j=1}^d (\mathbf{x}_b^j - \mathbf{x}_a^j)$ is the volume of the domain.

Loss functions and training We experimented with different loss functions such as `mse`, `mae` and cross-entropy to arrive at the surrogate f_w but did not notice significant differences in the convergence rate. We also experimented with standard training algorithms and found that optimizing using the Levenberg-Marquardt method and Bayesian Regularization perform better than conjugate gradient based methods particularly for discontinuous f .

Sampling Different estimates $\mu(\mathbf{w})$ may be drawn from the same samples $\{\mathbf{x}_n\}$ by either retraining the approximator network with different initialization conditions or due to the stochasticity in the optimization procedure. Although it is also possible to vary the samples across training runs (as with MC or QMC), we found that this did not impact estimation error, particularly for larger training data ($N > 32$). However, different sampling arrangements (correlations) with the same distribution were useful particularly when combined with control variates. e.g. Halton samples instead of random. Intuitively, this improves f_w thereby also improving the estimation error. This relationship requires further analysis and is a promising direction for future research.

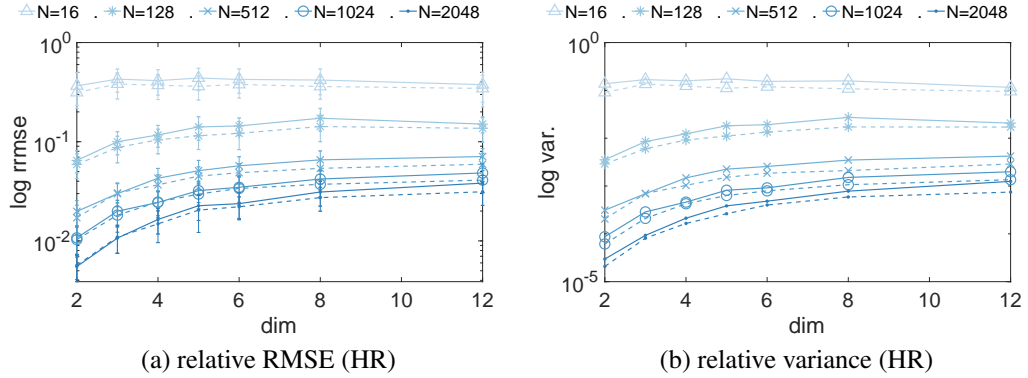


Figure 8: *Dimensionality* Relative error and variance across 120 randomly sampled HR integrands in $d = 2, 3, 4, 5, 6, 8$ and 12 (X-axes) for various amounts of training data N (different curves). The dashed lines show the same data when the number of neurons k is reduced by 50%.

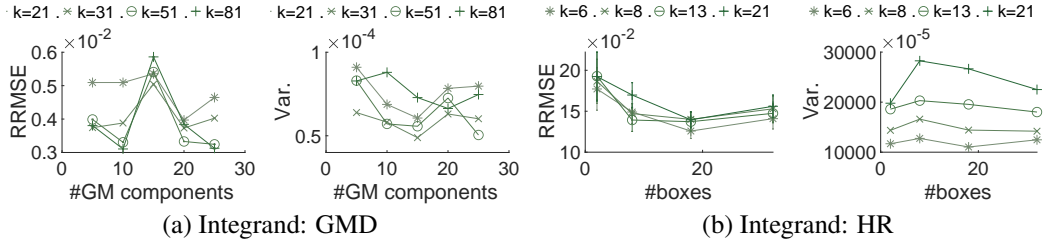


Figure 9: RMSE and variance using our method are consistent across integrands with different parameters. The plots in this figure visualize estimation error and variance using $N = 1024$ for various numbers of neurons k and integrand parameters. Curiously, the variance is higher for larger k .

Limitations and future work In our experiments, the choice of k had little impact on error for low training volumes ($N < 32$). For large N , its relevance depended on the nature of the integrand. For smooth integrands (GM), increasing k reduced error due to the improved approximation. For discontinuous integrands (GM, HR), increasing k arbitrarily was counterproductive (see fig. 9) due to increased error introduced by ‘ringing’ artifacts at discontinuities. This is an inherent limitation of shallow sigmoidal approximator networks which could be addressed by bounding width rather than depth [29] and adding layers. We strike a general compromise, for all experiments, choosing $k \propto N^{\frac{1}{1+d}}$ with a minimum of $k = 2$ neurons. Further investigation is required to extend our formula to multiple sigmoidal layers and to develop fast approximations of our exact formula.

5 Conclusion

We derived a formula, in closed-form, for the integral of a function represented by a one-layer feedforward neural network whose activation function is the logistic function. Our formula can be evaluated directly but also using a fixed-weight feedforward neural network with one layer. We call this network a Q-NET, and derived its weights and activation function. Q-NETs may be used to marginalize along input dimensions to yield functions in closed-form of the remaining dimensions. We presented experimental evidence to show that the error drops consistently (as the number of training samples for the approximator is increased) for challenging integrands, along with investigation of the effect of various parameters on the approximation.

A Appendix

A.1 Derivation

To derive the formula for the multidimensional case, we start with the simple case when $d = 1$ and $k = 1$, then develop intuition for $d = 2$ and finally generalize the result to d -dimensional integrands with k neurons in the hidden layer.

When $d = 1$, the matrix in equation 2 is reduced to a vector \mathbf{w}_1 ($k \times 1$). Further, when $k = 1$ (single neuron) all learned parameters for $f_{\mathbf{w}}$ reduce to scalars $w_1, w_2, b_1, b_2 \in \mathbb{R}$ so that

$$f_{\mathbf{w}}(x) = \frac{w_2}{1 + e^{-(w_1 x + b_1)}} + b_2, \quad x \in [-1, 1]$$

which can be integrated analytically to yield a formula for the integral of the approximate function:

$$\begin{aligned} \mu_{1,1}(\mathbf{w}) \equiv \int_{-1}^1 f_{\mathbf{w}}(x) dx &= \frac{w_2}{w_1} (\ln(1 + e^{w_1 + b_1}) - \ln(1 + e^{-w_1 + b_1})) + 2b_2 \end{aligned} \quad (7)$$

$$= \frac{w_2}{w_1} (\phi(w_1 + b_1) - \phi(-w_1 + b_1)) + 2b_2 \quad (8)$$

which consists of softplus terms $\phi(x) \equiv \ln(1 + e^x)$. Since the output layer is a linear combination of the activations of the neurons in the hidden layer, when $k > 1$ the rhs is the weighted sum:

$$\mu_{1,k}(\mathbf{w}) = \sum_{i=1}^k \frac{\mathbf{w}_2^i}{\mathbf{w}_1^i} [\phi(\mathbf{w}_1^i + \mathbf{b}_1^i) - \phi(-\mathbf{w}_1^i + \mathbf{b}_1^i)] + 2b_2, \quad (9)$$

where superscript i is used to denote the i^{th} element of a vector. Since μ_k is an exact integral of $f_{\mathbf{w}}$, it follows that if the approximation is accurate in the limit then the estimator is unbiased. i.e. $\langle f_{\mathbf{w}}(\mathbf{x}) \rangle = f(\mathbf{x}), \forall \mathbf{x} \in [-1, 1]^d$ implies $\langle \mu_{1,k} \rangle = I$. Since independent training runs of the approximator network result in different \mathbf{w} , secondary estimates of $\mu_{1,k}$ may be obtained by averaging training runs obtained with random initialization.

When $d = 2$ and $k = 1$, the approximator network can be written as $f_{\mathbf{w}} = w_2 \sigma(\mathbf{w}_1 \mathbf{x} + b_1) + b_2$ where $\mathbf{x} = [x_1, x_2]^T, w_2, b_1, b_2 \in \mathbb{R}$ and \mathbf{w}_1 is a 1×2 vector. Proceeding similarly to the 1D case we can first integrate over one variable x_1 (or equally x_2) and the intermediate formula, a function of x_2 (resp. x_1), requires a second integration step:

$$\begin{aligned} \mu_{2,1}(\mathbf{w}) &= \int_{-1}^1 \frac{w_2}{\mathbf{w}_1^1} [\phi(\mathbf{w}_1^1 + \mathbf{w}_1^2 x_2 + b_1) - \phi(-\mathbf{w}_1^1 + \mathbf{w}_1^2 x_2 + b_1)] dx_2 + \int_{-1}^1 2b_2 dx_2 \\ &= \frac{w_2}{\mathbf{w}_1^1 \mathbf{w}_1^2} [\text{Li}_2(\exp(\mathbf{w}_1^1 + \mathbf{w}_1^2 - b_1)) - \text{Li}_2(\exp(\mathbf{w}_1^1 - \mathbf{w}_1^2 - b_1)) \\ &\quad - \text{Li}_2(\exp(-\mathbf{w}_1^1 + \mathbf{w}_1^2 - b_1)) + \text{Li}_2(\exp(-\mathbf{w}_1^1 - \mathbf{w}_1^2 - b_1))] \\ &\quad + 4w_2 + 4b_2. \end{aligned} \quad (10)$$

Here $\text{Li}_d(x)$ represents the polylogarithm [?] function of order 2 and is real when x and s are real.

An important property of this function is that $\text{Li}_{d+1}(x) = \int_0^x \text{Li}_d(y)/y dy$, which enables the general

formula for the d -dimensional case with $k = 1$ hidden neuron:

$$\mu_{d,1}(\mathbf{w}) = w_2 \sum_{m=1}^{2^d} \frac{(-1)^{\alpha_m} \text{Li}_d(-\exp(S^{l,m} \mathbf{w}_1^\top - b_1))}{\prod_{j=1}^d \mathbf{w}_1^j} + 2^d w_2 + 2^d b_2$$

where the rows of $2^d \times d$ matrix S , where $S^{l,m} \in \{-1, 1\}$, represent all 2^d combinations of d signs, one for each element in the row vector \mathbf{w}_1 . The contribution of each Li_d term is either positive (α_m is even) or negative (α_m is odd) depending on whether there are an even (resp. odd) number of -1 s in the row $S^{l,:}$.

The general case $\mu_{d,k}(\mathbf{w})$, where the approximation is given by equation 2, is a weighted sum of the outputs of the k neurons ($\mathbf{v}^i, i = 1 \dots k$), with weights as the corresponding elements of \mathbf{w}_2 (eq. 3).

A.2 Error

When $f_{\mathbf{w}}$ is trained to approximate f , the approximation error of shallow feedforward networks [26, 4] is bounded by $\|f(\mathbf{x}) - f_{\mathbf{w}}(\mathbf{x})\|_2^2 < \epsilon$ where $\epsilon = \tilde{h}/k^{2c/d}$ when \tilde{h} is the first moment of the Fourier spectrum of function f which is c times differentiable. But

$$\|f(\mathbf{x}) - f_{\mathbf{w}}(\mathbf{x})\|_2^2 = \int_{\mathcal{D}} (f(\mathbf{x}) - f_{\mathbf{w}}(\mathbf{x}))^2 d\mathbf{x} \quad (11)$$

$$= \int_{\mathcal{D}} (f^2(\mathbf{x}) + f_{\mathbf{w}}^2(\mathbf{x}) - 2f(\mathbf{x})f_{\mathbf{w}}(\mathbf{x})) d\mathbf{x} \quad (12)$$

$$= \int_{\mathcal{D}} f^2(\mathbf{x}) d\mathbf{x} + \int_{\mathcal{D}} f_{\mathbf{w}}^2(\mathbf{x}) d\mathbf{x} - 2 \int_{\mathcal{D}} f(\mathbf{x})f_{\mathbf{w}}(\mathbf{x}) d\mathbf{x} \quad (13)$$

$$= V[f(\mathbf{x})] + V[f_{\mathbf{w}}(\mathbf{x})] + \left(\int_{\mathcal{D}} f(\mathbf{x}) d\mathbf{x} \right)^2 \quad (\mathbf{x} \text{ is uniform})$$

$$+ \left(\int_{\mathcal{D}} f_{\mathbf{w}}(\mathbf{x}) d\mathbf{x} \right)^2 - 2 \int_{\mathcal{D}} f(\mathbf{x})f_{\mathbf{w}}(\mathbf{x}) d\mathbf{x} \quad (14)$$

$$= V[f(\mathbf{x})] + V[f_{\mathbf{w}}(\mathbf{x})] + \left(\int_{\mathcal{D}} f(\mathbf{x}) d\mathbf{x} - \int_{\mathcal{D}} f_{\mathbf{w}}(\mathbf{x}) d\mathbf{x} \right)^2$$

$$+ 2 \int_{\mathcal{D}} f(\mathbf{x}) d\mathbf{x} \int_{\mathcal{D}} f_{\mathbf{w}}(\mathbf{x}) d\mathbf{x} - 2 \int_{\mathcal{D}} f(\mathbf{x})f_{\mathbf{w}}(\mathbf{x}) d\mathbf{x} \quad (15)$$

$$= V[f(\mathbf{x})] + V[f_{\mathbf{w}}(\mathbf{x})] + (I - \mu)^2 - 2\text{cov}[f(\mathbf{x}), f_{\mathbf{w}}(\mathbf{x})] \quad (15)$$

$$= V[f(\mathbf{x}) - f_{\mathbf{w}}(\mathbf{x})] + (I - \mu)^2 \quad (16)$$

which then gives us the result in the paper: $(I - \mu)^2 < \epsilon - V[f(\mathbf{x}) - f_{\mathbf{w}}(\mathbf{x})]$.

References

- [1] G. Cybenko, “Approximation by superpositions of a sigmoidal function,” *Mathematics of control, signals and systems* **2** no. 4, (1989) 303–314.
- [2] K. Hornik, “Approximation capabilities of multilayer feedforward networks,” *Neural networks* **4** no. 2, (1991) 251–257.
- [3] Z. Lu, H. Pu, F. Wang, Z. Hu, and L. Wang, “The expressive power of neural networks: A view from the width,” [arXiv:1709.02540 \[cs.LG\]](https://arxiv.org/abs/1709.02540).
- [4] U. Shaham, A. Cloninger, and R. R. Coifman, “Provable approximation properties for deep neural networks,” [arXiv:1509.07385 \[stat.ML\]](https://arxiv.org/abs/1509.07385).
- [5] A. B. Owen, *Monte Carlo theory, methods and examples*. 2013. <https://statweb.stanford.edu/~owen/mc/>.
- [6] R. Wan, M. Zhong, H. Xiong, and Z. Zhu, “Neural control variates for variance reduction,” [arXiv:1806.00159 \[stat.ML\]](https://arxiv.org/abs/1806.00159).
- [7] H. Brass and K. Petras, *Quadrature Theory: The Theory of Numerical Integration on a Compact Interval*. Mathematical surveys and monographs. American Mathematical Society.
- [8] V. Keshavarzzadeh, R. M. Kirby, and A. C. Narayan, “Numerical integration in multiple dimensions with designed quadrature,” *CoRR abs/1804.06501* (2018) , [arXiv:1804.06501](https://arxiv.org/abs/1804.06501).
- [9] N. Metropolis and S. Ulam, “The monte carlo method,” *Journal of the American Statistical Association* **44** no. 247, (1949) 335–341.

[10] H. Niederreiter, “Quasi-monte carlo methods and pseudo-random numbers,” *Bull. Amer. Math. Soc.* **84** no. 6, (11, 1978) 957–1041.

[11] H. Niederreiter, *Random Number Generation and Quasi-Monte Carlo Methods*.
<https://epubs.siam.org/doi/pdf/10.1137/1.9781611970081.fm>.

[12] P. Grohs, A. Jentzen, and D. Salimova, “Deep neural network approximations for monte carlo algorithms,” [arXiv:1908.10828 \[math.NA\]](https://arxiv.org/abs/1908.10828).

[13] Z. Ghahramani and C. E. Rasmussen, “Bayesian monte carlo,” in *Advances in Neural Information Processing Systems 15*, S. Becker, S. Thrun, and K. Obermayer, eds., pp. 505–512. MIT Press, 2003.

[14] M. Osborne, R. Garnett, Z. Ghahramani, D. K. Duvenaud, S. J. Roberts, and C. E. Rasmussen, “Active learning of model evidence using bayesian quadrature,” in *Advances in Neural Information Processing Systems 25*, pp. 46–54. 2012.

[15] M. Kanagawa and P. Hennig, “Convergence guarantees for adaptive bayesian quadrature methods,” in *Advances in Neural Information Processing Systems 32*, pp. 6237–6248. Curran Associates, Inc., 2019.

[16] B. Shahriari, K. Swersky, Z. Wang, R. P. Adams, and N. de Freitas, “Taking the human out of the loop: A review of bayesian optimization,” *Proceedings of the IEEE* **104** no. 1, (2016) 148–175.

[17] F.-X. Briol, C. Oates, M. Girolami, and M. A. Osborne, “Frank-wolfe bayesian quadrature: Probabilistic integration with theoretical guarantees,” in *Advances in Neural Information Processing Systems 28*, C. Cortes, N. D. Lawrence, D. D. Lee, M. Sugiyama, and R. Garnett, eds., pp. 1162–1170. 2015.

[18] T. Gunter, M. A. Osborne, R. Garnett, P. Hennig, and S. J. Roberts, “Sampling for inference in probabilistic models with fast bayesian quadrature,” in *Proceedings of the 27th International Conference on Neural Information Processing Systems - Volume 2*, NIPS’14, p. 2789–2797. MIT Press, Cambridge, MA, USA, 2014.

[19] K. Kandasamy, J. Schneider, and B. Póczos, “Bayesian active learning for posterior estimation,” in *Proceedings of the 24th International Conference on Artificial Intelligence*, IJCAI’15, p. 3605–3611. AAAI Press, 2015.

[20] H. Wang and J. Li, “Adaptive gaussian process approximation for bayesian inference with expensive likelihood functions,” *Neural Computation* **30** no. 11, (2018) 3072–3094, https://doi.org/10.1162/neco_a_01127. PMID: 30216145.

[21] L. Acerbi, “Variational bayesian monte carlo,” in *Advances in Neural Information Processing Systems 31*, S. Bengio, H. M. Wallach, H. Larochelle, K. Grauman, N. Cesa-Bianchi, and R. Garnett, eds., pp. 8223–8233. 2018.

[22] T. Karaletsos and T. D. Bui, “Hierarchical gaussian process priors for bayesian neural network weights,” 2020.

[23] A. Dereventsov, A. Petrosyan, and C. Webster, “Neural network integral representations with the relu activation function,” [arXiv:1910.02743 \[cs.LG\]](https://arxiv.org/abs/1910.02743).

[24] L. Euler, *Institutionum calculi integralis volumen primum*, vol. 1. 1768.
<https://epubs.siam.org/doi/pdf/10.1137/1.9781611970081.fm>.

[25] L. Lewin, *Polylogarithms and associated functions*. North Holland, 1981.

[26] A. R. Barron, “Universal approximation bounds for superpositions of a sigmoidal function,” *IEEE Transactions on Information theory* **39** no. 3, (1993) 930–945.

[27] K. Subr and J. Kautz, “Fourier analysis of stochastic sampling strategies for assessing bias and variance in integration,” *ACM Trans. Graph.* **32** no. 4, (July, 2013) .
<https://doi.org/10.1145/2461912.2462013>.

[28] L. Belcour, C. Soler, K. Subr, N. Holzschuch, and F. Durand, “5d covariance tracing for efficient defocus and motion blur,” *ACM Trans. Graph.* **32** no. 3, (July, 2013) .
<https://doi.org/10.1145/2487228.2487239>.

[29] F. Fan, D. Wang, H. Guo, Q. Zhu, P. Yan, G. Wang, and H. Yu, “Slim, sparse, and shortcut networks,” [arXiv:1811.09003 \[cs.LG\]](https://arxiv.org/abs/1811.09003).